JOURNAL OF GUIDANCE, CONTROL, AND DYNAMICS
Vol. 17, No. 3, May–June 1994

Separation Dynamics of Ullage Rockets

Rajeev Lochan and V. Adimurthy
Vikram Sarabhai Space Center, Trivandrum 695 022, India
and
K. Kumar
Indian Institute of Technology, Kanpur 208 016, India

The dynamics associated with the jettisoning of spent ullage rocket systems from the parent launch vehicle is investigated. The analysis considers a spring-based mechanism employed to jettison the system hinged on to an accelerating stage. Closed-form solutions are obtained. Analytical expressions are developed for the hinge reactions. Conditions are derived for optimum separation velocity and guidelines presented for selection of design parameters. The influence of residual thrust of ullage rockets on the separation process is examined and the expressions for its permissible value developed.

Nomenclature

a	= constant longitudinal acceleration of the thrusting stage
b	= distance of the nozzle throat from the hinge (Fig. 1)
E	= net stored spring energy
h	= longitudinal distance between the spring and the hinge (Fig. 1)
I_0, I_c	= X_3-mass moment of inertia of the spent ullage system about the hinge, and its own mass center, respectively
k	= effective stiffness of the springs
ℓ	= distance of the mass center from the hinge (Fig. 1)
M	= moment about the hinge due to the residual thrust
m	= mass of the spent ullage system
M_{c1}, M_{c2}, M_{c3}	= critical values of the moments about the hinge, Eqs. (26), (30), and (34)
$\hat{M}_{c1}, \hat{M}_{c2}, \hat{M}_{c3}$	= normalized critical values of the moments, $\hat{M}_{ci} = M_{ci}/(ma\ell)$, $i = 1, 2, 3$
R_1, R_2	= lateral and longitudinal hinge reactions (Fig. 1)

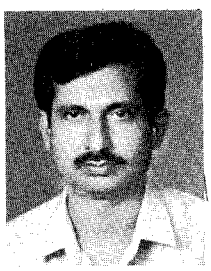

Rajeev Lochan graduated with a degree in mechanical engineering from BIT Sindri (Bihar), India, in 1973 and received his Master's in aeronautical engineering from the Indian Institute of Technology (IIT) Kanpur in 1976. He participated in the development of a trisonic wind tunnel at IIT Kanpur before joining Vikram Sarabhai Space Center (VSSC) Trivandrum, in 1977. Since then, he has been engaged in the research of diverse aspects of flight mechanics of launch vehicles. Dynamics of separating bodies, deployment dynamics, boost phase guidance, and onboard algorithms for position and attitude determination are some of the areas where he has made contributions. Currently he is pursuing his doctorate in aerospace engineering at IIT Kanpur in addition to his present responsibilities in the Aerodynamics Division of VSSC.

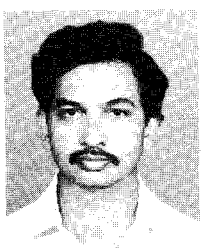

V. Adimurthy is Head of the Aerodynamics Division at Vikram Sarabhai Space Center. Born in 1946 in Rajahmundry, India, he was educated at Andhra University in Waltair, and later at the Indian Institute of Technology Kanpur, where he received his Ph.D. in 1973. He was a Research Fellow of the Alexander von Humboldt Foundation during 1979–80 at Stuttgart University, Germany. His contributions are in the areas of aerodynamics, flight mechanics, and trajectory optimization of aerospace vehicles.

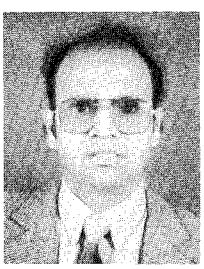

K. Kumar was born in India on November 19, 1946. He received a B.Sc. from the University of Allahabad, India, in 1964, a B. Tech. degree in mechanical engineering from IIT Kharagpur, India, in 1968, and a Ph.D. for work in satellite attitude dynamics and control from the University of British Columbia, Canada, in 1972. He is presently a Professor in the Department of Aerospace Engineering at the Indian Institute of Technology, Kanpur, India. His current research interests include dynamics and control of aerospace vehicles, static deformation of cables, optimization, and filtering.

Received March 29, 1992; revision received June 9, 1993; accepted for publication June 27, 1993.

$\hat{R}_1, \hat{R}_2$ = normalized hinge reactions, $\hat{R}_i = R_i/(ma)$, $i = 1, 2$
T = constant residual thrust
t = time since initiation of separation
T_{c1}, T_{c2}, T_{c3} = critical values of residual thrusts corresponding to the moments M_{c1}, M_{c2}, and M_{c3}, respectively
u_1, u_2 = lateral and longitudinal velocities at $t = \tau_2$, i.e., the end of phase II
v_1, v_2 = X_1 and X_2 components of the instantaneous relative velocity of the mass center of the ullage system with respect to the thrusting stage, respectively
X_1X_2 = uniformly accelerating frame of reference fixed with the thrusting stage (Fig. 1)
x_1, x_2 = instantaneous displacement of the spent ullage mass center referred to X_1X_2 frame
α = nozzle cant angle of the ullage rocket (Fig. 1)
β, ε = angles describing locations of center of mass and the nozzle throat, respectively (Fig. 1)
δ = precompression of the springs
ζ = dependent energy ratio parameter, Eq. (20)
$\eta_1, \eta_2, \eta_3, \eta_4$ = independent frequency parameters, Eqs. (3), (17b), and (28b)
Θ = amplitude of oscillations, Eq. (28a)
θ = angle θ between the longitudinal axis of the ullage system and that of the thrusting stage (Fig. 1)
θ_1 = angle θ at which the springs relax completely, also called first angle, Eq. (4)
θ_2 = angle θ at which the ullage system gets released from the hinge, also called second angle
$\bar{\theta}$ = angle θ at which angular rate $\omega = 0$
ν = frequency of oscillation, Eq. (29)
ξ = independent dimensionless parameter, Eq. (17a)
τ_1, τ_2 = time instants at which $\theta = \theta_1$ and $\theta = \theta_2$, respectively
ω = angular velocity
ω_1, ω_2 = angular velocities at $\theta = \theta_1$ and $\theta = \theta_2$, respectively

Superscripts

$( )^*$ = ( ) under optimum conditions
$(\dot{})$ = time derivative

Introduction

LARGE liquid fueled rocket engines often demand a positive longitudinal acceleration for their own initiation when utilized as an intermediate stage. A number of small solid rockets with relatively low thrust and short burn time, called ullage rockets, strapped on to the liquid stage may be used for this purpose. These provide low accelerations causing liquid propellants to settle over the tank outlets ensuring an adequate fuel supply for main engine startup. After the successful initiation, however, the spent rockets may be jettisoned for better performance. The spring-based systems achieve this separation by commanding release of the precompressed springs. The European launch vehicle Ariane has successfully utilized such separation systems for discarding the ullage rockets. A judicious jettisoning system design must not only ensure collision-free separation but also limit the resulting disturbances on the liquid stage to a minimum. This paper analyzes the dynamics involved in the separation of ullage rockets from the launch vehicle.

The dynamics of separating bodies has received the attention of several investigators. Chubb[1] constructed collision boundaries between two separating stages. Dwork[2] and Wilke[3] provide valuable insight into disturbances caused by separation mechanisms in a spinning setup. Waterfall[4] investigated multispring systems for separation of spinning and nonspinning bodies. Longren[5] analyzed spin-stabilized rockets with guide shoes and rails constraining the lateral motion. Subramanyam[6] developed a general model for spring-assisted stage separation. Lochan et al.[7,8] examined a multi-

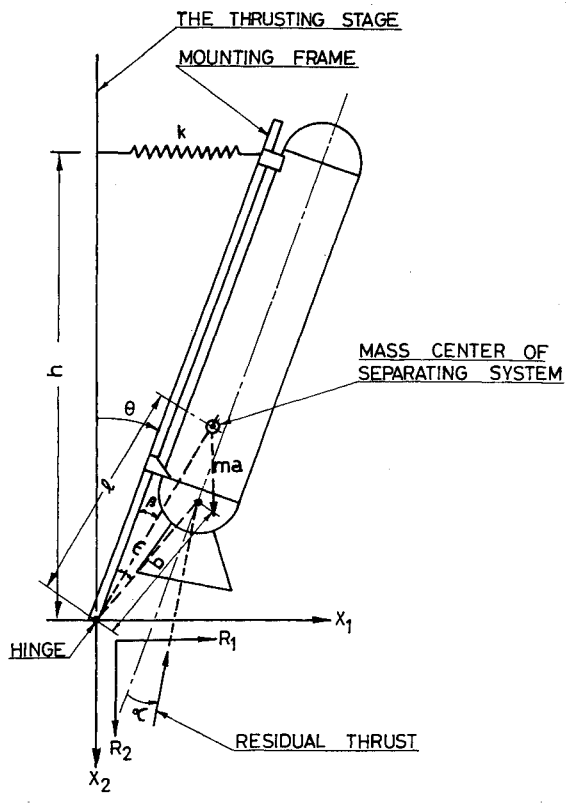

Fig. 1 Typical model of ullage separation system.

step separation where a set of passenger payloads separate from one another. Through analysis of the separation of apogee motor from payload, Biswas[9] indicated the possibility of an increase in lifetime by nonseparation. Sundaramurthy et al.,[10] Biswas,[11] and Prahlad[12] investigated several aspects of separation of strap ons from the launch vehicle. Analyzing the same problem, the authors[13] have examined geometry of collision and constructed the no-collision domain in design parameter space. The specific problem of separation of spent ullage rockets, however, has not been addressed.

The dynamics of ullage rocket separation can differ significantly from that of the other separating bodies. Unlike the general stage separation, the spent system is usually hinged on to the core. Furthermore, the separation of ullage rockets can be accompanied by a significant lateral velocity component. The requirement of providing adequate initial acceleration preceding the ignition of the liquid stage is met through several sets of small ullage rockets placed symmetrically on the surface of the launch vehicle. Each of these sets may have one or more ullage rockets. A commonly used separation setup is shown in Fig. 1. Here, a set of rockets is mounted over a frame whose lower ends are hinged on to the surface of the accelerating stage. The upper ends are mounted through thrust transfer brackets and held in position using ball-lock mechanisms. Precompressed springs supply the necessary energy for separation. Under the action of springs and the acceleration of the stage, the entire spent ullage system rotates about the hinge. However, after rotating by a fixed prespecified angle, these get released from the hinge, and their subsequent motion is free from constraints. The analysis may be further complicated by residual thrust. Although a number of countries have used liquid engine technology for years, no related investigations appear to have been reported in open literature. This paper represents a systematic attempt to analyze the problem of ullage rocket separation.

Formulation

We now attempt to formulate the equations for the ullage rockets in various phases of motion. In view of the nonspinning main stage and the typical in-plane layout of the spring-hinge-ullage system, the planar dynamics analysis is undertaken. The impor-

tance of such a simplified approach in providing insight to help designers select preliminary design parameters cannot be overemphasized. Although the present analysis holds for any number of springs, all are assumed to be at the same longitudinal distance h from the hinge and to have the same precompression δ.

External forces and moments are a consequence of gravitational pull, aerodynamic effects, thrust, residual thrust, and the forces induced by the separation mechanisms. Since our interest lies in the relative motion of the ullage system with respect to the main stage over short durations (typically around 1 s), gravitational forces have little effect and are neglected. For the same reason, for an ideally controlled thrusting stage, the acceleration vector is essentially constant and remains parallel to the longitudinal axis. Finally, since liquid stage ignition occurs at high altitudes where aerodynamic forces are small, these too have been ignored.

Let us define a frame of reference X_1X_2 attached at the hinge and accelerating with the liquid stage. Here, the X_2 axis is taken along the longitudinal axis and the X_1 axis lies in the plane of separation normal to the X_2 axis. This frame being noninertial, the equations of motion require inclusion of D'Alembert force ma as shown in Fig. 1. The system undergoes three distinct phases of motion: 1) phase I in which both the spring and hinge are active, 2) phase II wherein the spring is relaxed but the hinge constraint remains, and 3) phase III after the ullage rocket gets detached from the core.

Phase I ($0 \le t \le \tau_1$ and $0 \le \theta \le \theta_1$)

This phase begins with the separation process and ends when the spring attains its free nominal length.

The precompression of the spring being small, the angle θ may be assumed to be small in this phase and the spring force can be taken to be parallel to the X_1 axis. Its governing equation of motion can be written as

$$\ddot{\theta} + [(kh^2 - ma\ell \cos\beta)/I_0]\theta = (kh\delta + ma\ell \sin\beta)/I_0 \qquad (1)$$

the initial conditions being

$$\theta = \dot{\theta} = 0 \qquad \text{at} \qquad t = 0$$

This equation may be written in more convenient form as

$$\ddot{\theta} + (\eta_1^2 - \eta_2^2 \cos\beta)\,\theta = \theta_1 \eta_1^2 + \eta_2^2 \sin\beta \qquad (2)$$

where the frequency parameters η_1 and η_2 can be attributed to the presence of spring and the core acceleration, respectively,

$$\eta_1 = \sqrt{kh^2/I_0} \qquad (3a)$$

Table 1 Parameter values and basic results for an ullage system having two rockets

I. Physical system parameters	
Mass of the complete spent ullage system, kg	75
System moment of inertia about mass center, I_c, kgm^2	15
Distance of the springs from the hinge h, m	1.25
Effective spring stiffness k, kN/m	20
Spring precompression δ, mm	75
Acceleration of the liquid stage, a, m/s^2	15
Second angle θ_2, deg	70
Nozzle cant angle α, deg	10
Location of the center of mass of the separating system ℓ, m	0.6
and β, deg	12
Location of the nozzle throat b, m	0.4
and ε, deg	17
II. Related design parameters	
$\theta_1 = 0.06$; $\theta_2 = 1.22$; $\beta = 0.21$; $\eta_1 = 27.28$ s^{-1}	
$\eta_2 = 4.01$ s^{-1}; $\eta_3 = 5.0$ s^{-1}; $\xi = 1.33$; $\zeta = 12.0$	
III. Some basic results	
$\tau_1 = 54.9$ ms; $\omega_1 = 101.5$ deg/s; $\tau_2 = 414.5$ ms; $\omega_2 = 311.96$ deg/s	
$u_1 = 0.45$ m/s; $u_2 = 3.23$ m/s; $\theta_2^* = 32.956$ deg; $u_1^* = 1.432$ m/s	
$M_{c1} = 2051$ Nm; $M_{c2} = 1098$ Nm; $M_{c3} = 406$ Nm	
$T_{c1} = 11{,}098$ N; $T_{c2} = 6044$ N; $T_{c3} = 2237$ N	

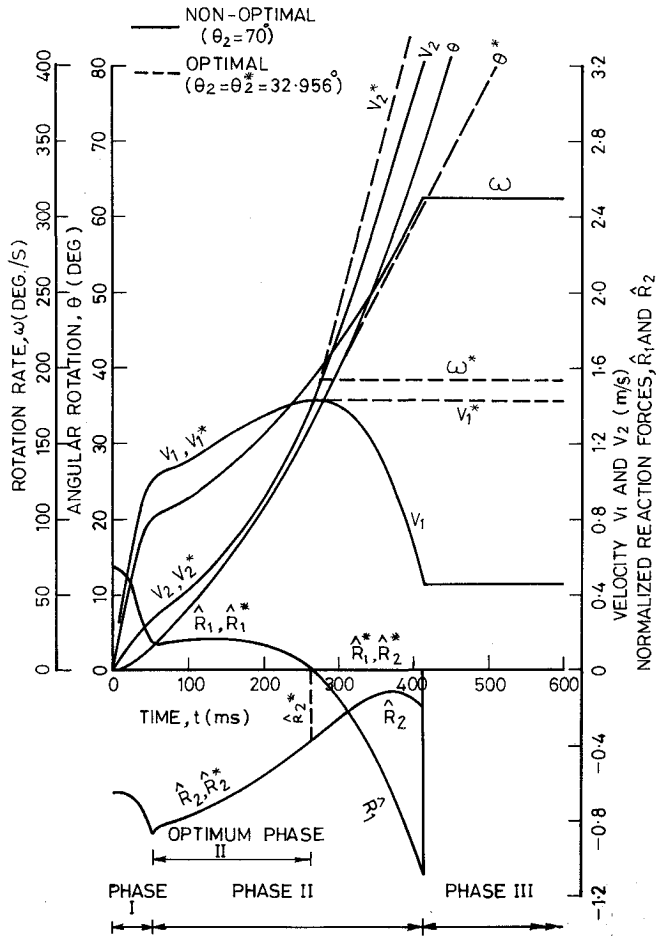

Fig. 2 Plots showing time history of system variables: β = 12 deg.

$$\eta_2 = \sqrt{ma\ell/I_0} \qquad (3b)$$

The angle θ_1 at which the spring gets relaxed completely marking the end of the phase I—hereafter referred to as the first angle—is given by

$$\theta_1 = \frac{\delta}{h} \qquad (4)$$

Since in practical systems $\eta_1 \gg \eta_2$, the system invariably behaves as a simple harmonic oscillator, the solution for which can be stated simply as follows:

$$\theta = \left(\frac{\theta_1\eta_1^2 + \eta_2^2 \sin\beta}{\eta_1^2 - \eta_2^2\cos\beta}\right)\left\{1 - \cos\left(t\sqrt{\eta_1^2 - \eta_2^2\cos\beta}\right)\right\} \qquad (5a)$$

$$\dot{\theta} = \left(\frac{\theta_1\eta_1^2 + \eta_2^2 \sin\beta}{\sqrt{\eta_1^2 - \eta_2^2\cos\beta}}\right)\sin\left(t\sqrt{\eta_1^2 - \eta_2^2\cos\beta}\right) \qquad (5b)$$

At the instant τ_1 marking the end of phase I given by

$$\tau_1 = \{\eta_1^2 - \eta_2^2\cos\beta\}^{-1/2}\cos^{-1}\left\{\frac{\eta_2^2(\sin\beta + \theta_1\cos\beta)}{\theta_1\eta_1^2 + \eta_2^2\sin\beta}\right\} \qquad (6)$$

the angular velocity of the spent ullage system can be obtained as

$$\omega_1 = \{(\eta_1^2 + \eta_2^2\cos\beta)\theta_1^2 + 2\theta_1\eta_2^2\sin\beta\}^{1/2} \qquad (7)$$

The expressions for the relative velocity components are

$$v_1 = \dot{\theta}\ell \cos(\theta + \beta) \tag{8a}$$

$$v_2 = \dot{\theta}\ell \sin(\theta + \beta) \tag{8b}$$

Phase II ($\tau_1 \le t \le \tau_2$ and $\theta_1 \le \theta \le \theta_2$)

In this phase, say, $\tau_1 \le t \le \tau_2$ and $\theta_1 \le \theta \le \theta_2$, the spring is relaxed and the angle θ need not be small. The angle θ_2 is an important design parameter signaling the release of the spent system from the hinge and will hereafter be referred to as the second angle. The equation of motion now takes the form

$$\ddot{\theta} = \eta_2^2 \sin(\theta + \beta) \tag{9}$$

The initial conditions become

$$\theta = \theta_1 \quad \text{and} \quad \omega = \omega_1 \quad \text{at} \quad t = \tau_1$$

Equation (9) when integrated leads to

$$\omega = \dot{\theta} = \left[\eta_1^2\theta_1^2 + 2\eta_2^2\{\cos\beta - \cos(\theta + \beta)\}\right]^{1/2} \tag{10}$$

The temporal behavior is obtained in terms of the integral relation

$$t = \tau_1 + \int_{\theta_1}^{\theta} \left[\eta_1^2\theta_1^2 + 2\eta_2^2\{\cos\beta - \cos(\theta + \beta)\}\right]^{-1/2} d\theta \tag{11}$$

At the end of the second phase, the relative lateral and longitudinal velocity components can be easily evaluated

$$u_1 = \left[\eta_1^2\theta_1^2 + 2\eta_2^2\{\cos\beta - \cos(\theta_2 + \beta)\}\right]^{1/2}\ell \cos(\theta_2 + \beta) \tag{12a}$$

$$u_2 = \left[\eta_1^2\theta_1^2 + 2\eta_2^2\{\cos\beta - \cos(\theta_2 + \beta)\}\right]^{1/2}\ell \sin(\theta_2 + \beta) \tag{12b}$$

Phase III ($t > \tau_2$ and $\theta > \theta_2$)

In this phase, having broken loose from the core, the ullage system moves freely, and its motion can be simply described as

$$\ddot{\theta}_2 = 0 \tag{13a}$$

$$\dot{v}_1 = 0 \tag{13b}$$

$$\dot{v}_2 = a \tag{13c}$$

The terminal conditions of phase II constitute the initial conditions for this phase. The integration of the preceding relations leads to the following solution

$$\theta = \theta_2 + \omega_2(t - \tau_2), \qquad \omega = \omega_2 \tag{14a}$$

$$x_1 = \ell \sin(\theta_2 + \beta) + u_1(t - \tau_2), \qquad v_1 = \omega_2\ell \cos(\theta_2 + \beta) \tag{14b}$$

$$x_2 = -\ell \cos(\theta_2 + \beta) + u_2(t - \tau_2) + (1/2)a(t - \tau_2)^2$$
$$v_2 = \omega_2\ell \sin(\theta_2 + \beta) + a(t - \tau_2) \tag{14c}$$

It may be observed here that the complete dynamics may be described in terms of the three angles β, θ_1, and θ_2 and the two frequency parameters η_1 and η_2.

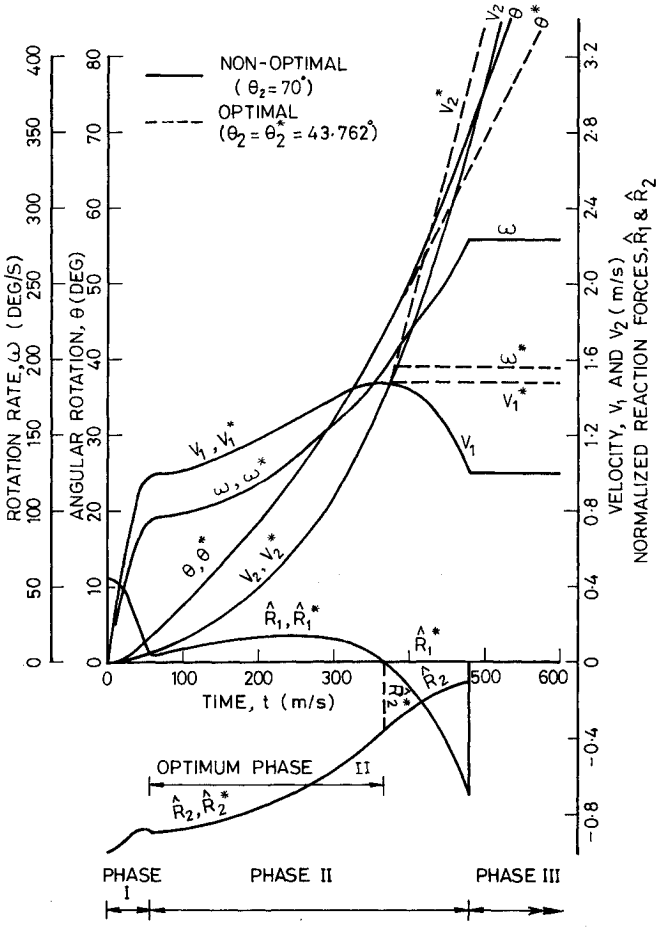

Fig. 3 Plots showing time history of system variables: $\beta = 0$ deg.

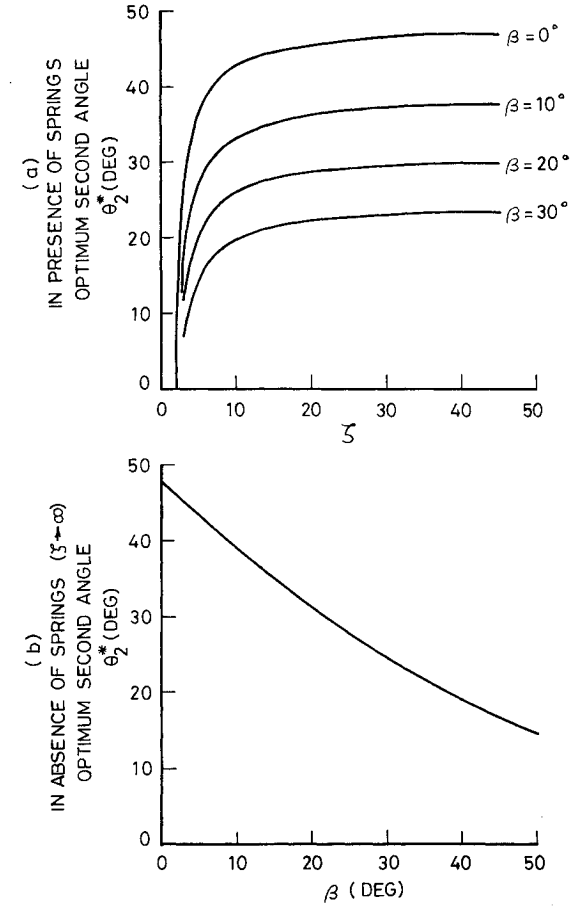

Fig. 4 Behavior of optimum second angle as influenced by ζ and β: a) in the presence of springs and b) in the absence of springs.

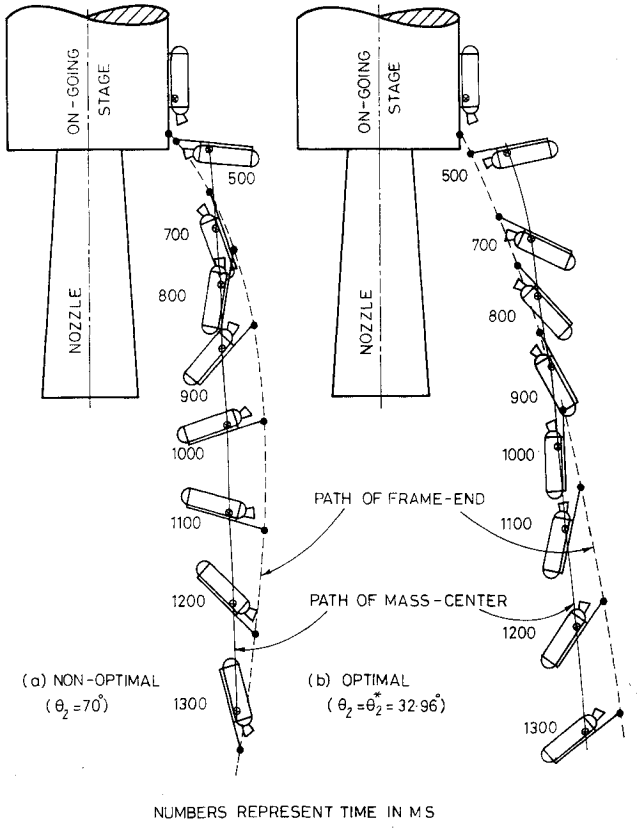

Fig. 5 Schematic representation of falling ullage system: a) nonoptimal and b) optimal.

Constraint Forces

It is now easy to evaluate the hinge reactions R_1 and R_2 during the first two phases using the relations

$$R_1 = m\dot{v}_1 - k(\delta - h\theta); \qquad 0 \le t \le \tau_1$$
$$= m\dot{v}_1; \qquad \tau_1 \le t \le \tau_2 \tag{15a}$$

$$R_2 = m\dot{v}_2 - ma; \qquad 0 \le t \le \tau_2 \tag{15b}$$

whereas, the constraint forces are absent in phase III.

The corresponding normalized reactions $\hat{R}_1$ and $\hat{R}_2$ are given by

$$\hat{R}_1 = R_1/(ma) = (1/\eta_3^2)\cos(\theta+\beta)\{\theta_1\eta_1^2 + \eta_2^2 \sin\beta - (\eta_1^2 - \eta_2^2\cos\beta)\theta\} - (\dot{\theta}/\eta_3)^2\sin(\theta+\beta) - \xi(1 - \theta/\theta_1); \quad 0 \le t \le \tau_1$$
$$= (1/\eta_3^2)\{\eta_2^2\cos(\theta+\beta) - \dot{\theta}^2\}\sin(\theta+\beta); \qquad \tau_1 \le t \le \tau_2 \tag{16a}$$

$$\hat{R}_2 = R_2/(ma) = (1/\eta_3^2)\sin(\theta+\beta)\{\theta_1\eta_1^2 - \eta_2^2\sin\beta - (\eta_1^2 - \eta_2^2\cos\beta)\theta\} + (\dot{\theta}/\eta_3)^2\cos(\theta+\beta) - 1; \quad 0 \le t \le \tau_1$$
$$= (1/\eta_3^2)\{\eta_2^2\sin^2(\theta+\beta) + \dot{\theta}^2\cos(\theta+\beta)\} - 1; \quad \tau_1 \le t \le \tau_2 \tag{16b}$$

where the dimensionless parameter ξ and the dimensional parameter η_3 are given by

$$\xi = \frac{k\delta}{ma} \tag{17a}$$

$$\eta_3 = \sqrt{a/\ell} \tag{17b}$$

Optimality Condition

Among the various design parameters governing the dynamics, only a few can be chosen by a separation mechanism designer. These are spring energy E governed by the stiffness k and precompression δ, the second angle θ_2, and the placement h of the springs. Evidently, it would be desirable to select θ_2 so as to maximize the separation velocity u_1 as defined by Eq. (12a). The governing optimality condition is obtained as

$$\theta_2^* = \arccos\{(\eta_1^2\theta_1^2 + 2\eta_2^2\cos\beta)/(3\eta_2^2)\} - \beta \tag{18}$$

In general, this expression can be written in simpler form as

$$\theta_2^* = \arccos\{(2 + 2\zeta\cos\beta)/(3\zeta)\} - \beta \tag{19}$$

where

$$\zeta = \eta_2^2/[(1/2)\eta_1^2\theta_1^2] = ma\ell/[k(1/2)\zeta^2] \tag{20}$$

The parameter ζ is a dimensionless parameter and signifies the relative importance of work associated with longitudinal acceleration as compared to that of spring energy. However, it is not an independent parameter as is evident from the relation (20). The closed-form expression thus developed is of considerable significance as it provides the requisite design value for the second angle θ_2 as a function of the other system parameters.

The resulting optimal angular rate and separation velocity at the end of phase II are then given by

$$\omega_2^* = \sqrt{(\eta_1^2\theta_1^2 + 2\eta_2^2\cos\beta)/3} \tag{21a}$$

$$u_1^* = (\eta_1^2\theta_1^2 + 2\eta_2^2\cos\beta)^{3/2}\ell/(3\sqrt{3}\eta_2^2) = (2/3)^{3/2}(E + ma\ell\cos\beta)^{3/2}/(ma\sqrt{I_0}) \tag{21b}$$

Interestingly, neither the optimality condition nor the optimum separation velocity depend on h as long as θ_1 remains small as assumed at the outset. This deduction is also important as it enables a degree of flexibility in the system layout.

Separation without Springs

If the thrusting stage has sufficient acceleration and the angle $\beta > 0$, a clean separation may be achieved even without springs. Here, the "sufficient" acceleration level is decided by the geometry and the margins. More specifically, it would depend on the location of the surface that could possibly be struck by the ullage rockets. It may be established by graphic simulation of motion of these spent minirockets for preselected levels of the minimum geometric clearance. Now, considering the case when the springs are not employed, phase I vanishes altogether, and the equations governing the second phase hold throughout the domain $0 \le t \le \tau_2$. However, the parameter η_1 is now zero, and new initial conditions become

$$\theta = \dot{\theta} = 0 \qquad \text{at} \qquad t = 0$$

whereas the optimal condition simplifies to

$$\theta_2^* = \arccos\{(2/3)\cos\beta\} - \beta \tag{22}$$

and the corresponding separation velocity is

$$u_1^* = \{(2/3)\cos\beta\}^{3/2}\eta_2\ell \tag{23}$$

Influence of Leftover Thrust

Although the separation event usually occurs well after the burnout of the ullage rockets, there may still be some residual

thrust. Here, its influence is investigated and an attempt is made to estimate the thrust level that can be allowed without jeopardizing the separation process. Needless to say, incorporating this additional effect modifies the governing equations of motion in all three phases.

Phase I

The equation of motion in phase I may be written as

$$I_0\ddot{\theta} + (kh^2 - ma\ell\cos\beta)\theta = kh\delta + ma\ell\sin\beta - M \tag{24}$$

The initial conditions, however, remain unaltered. The moment M caused due to tail-off thrust T assumed to be constant can be written as

$$M = Tb\sin(\alpha + \varepsilon) \tag{25}$$

The condition for the separation motion to get initiated as evident from the right-hand side in Eq. (24) can be written as

$$kh\delta + ma\ell\sin\beta - M \geq 0$$

This can be restated as, say

$$M < kh\delta + ma\ell\sin\beta = M_{c1} \tag{26}$$

Under these conditions enabling initiation of separation, the solution for θ can be expressed as

$$\theta = 1/2\,\Theta\left\{1 - \cos\left(t\sqrt{\eta_1^2 - \eta_2^2\cos\beta}\right)\right\} \tag{27}$$

where

$$\Theta = 2\{\theta_1\eta_1^2 + \eta_2^2\sin\beta - \eta_4^2\}/\{\eta_1^2 - \eta_2^2\cos\beta\} \tag{28a}$$

$$\eta_4 = \sqrt{M/I_0} \tag{28b}$$

A new frequency parameter η_4 introduces the influence of the thrust moment. The resulting oscillation frequency is given by

$$\nu = \sqrt{\eta_1^2 - \eta_2^2\cos\beta} \tag{29}$$

The maximum θ, which is equal to Θ itself, should be greater than θ_1 if the spring is to reach the state of complete relaxation. And, in that case, the moment when the angle θ_1 is attained signals the release of spring from the latch and, hence, the end of the first phase. Otherwise, we simply have a situation of angle θ persistently oscillating between 0 and Θ.

Using Eq. (28a), the condition for the spring release to occur as is desirable can be simply stated as

$$\chi > \theta_1$$

which in turn leads to, say,

$$M < 1/2\{kh\delta + 2ma\ell\sin\beta + ma\ell\theta_1\cos\beta\} = M_{c2} \tag{30}$$

Needless to say, the spring having separated has no role in the subsequent dynamics. However, moment due to the residual thrust especially if large can cause the return of the ullage system toward the core ending up in unwanted collision between the two.

To develop the criterion for avoiding such a situation, one needs to examine the dynamics of the second phase.

Phase II

The modified equation of motion duly accounting for the residual thrust is obtained as

$$\ddot{\theta} = \eta_2^2\sin(\theta + \beta) - \eta_4^2 \tag{31}$$

Integrating it once with respect to time results in the following expression for the angular velocity:

$$\omega = \pm\sqrt{\eta_1^2\theta_1^2 + 2\eta_2^2\cos\beta - 2\eta_2^2\cos(\theta + \beta) - 2\eta_4^2\theta} \tag{32}$$

The problem of developing the criterion of avoiding collision gets highly simplified if we first find the angle at which the angular velocity becomes zero. This angle, referred to as $\bar{\theta}$ [as deduced from Eq. (32)], is given by

$$2\eta_2^2\cos(\bar{\theta} + \beta) + 2\eta_4^2\bar{\theta} = \eta_1^2\theta_1^2 + 2\eta_2^2\cos\beta \tag{33}$$

It is now easy to see that if the thrust moment is less than the moment due to the inertial force (ma) at $\theta = \bar{\theta}$, a clean separation is expected during the subsequent motion. Hence, we require, say

$$M \leq ma\ell\sin(\bar{\theta} + \beta) = M_{c3}$$

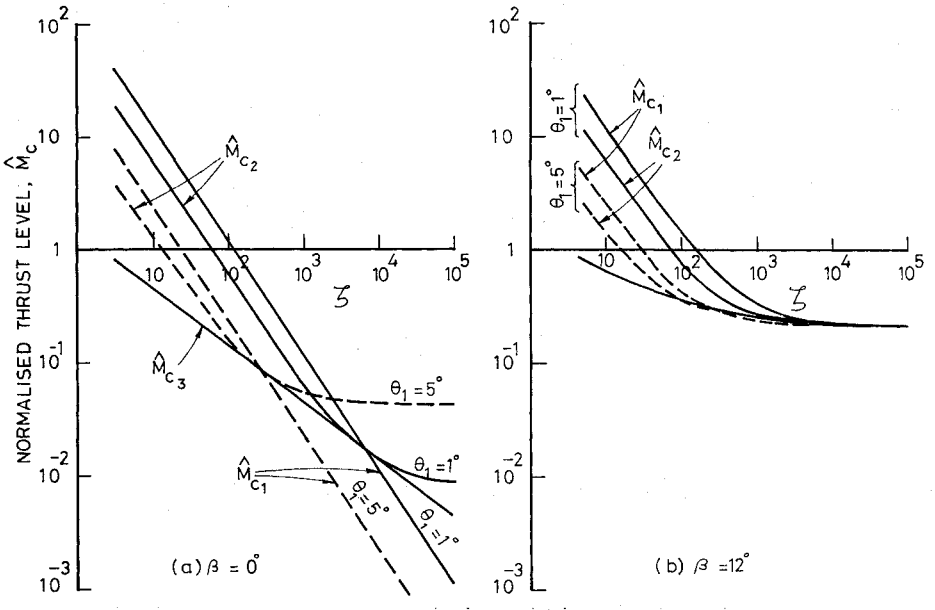

Fig. 6 Critical moment levels due to residual thrust.

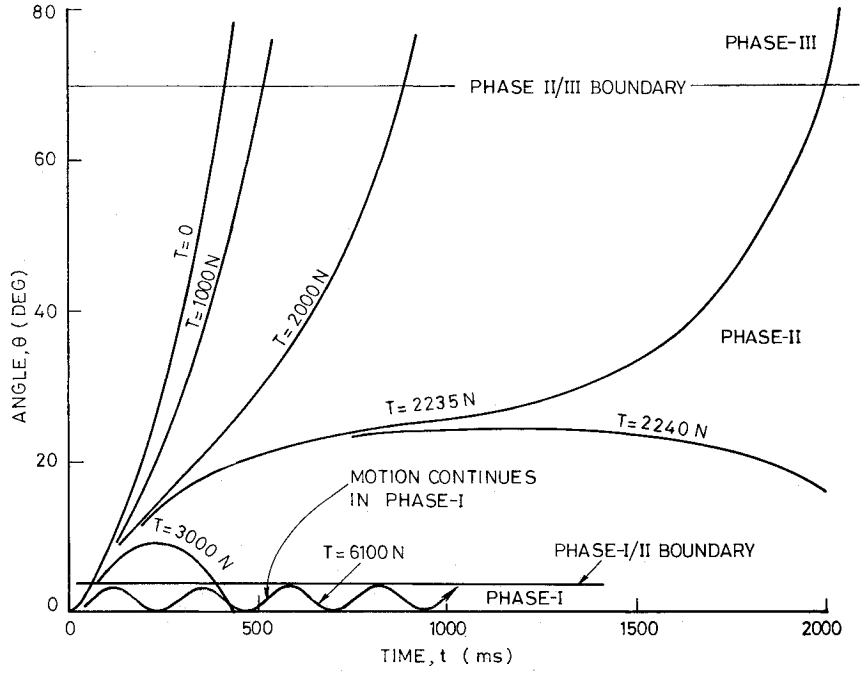

Fig. 7 Influence of residual thrust on evolution of angle θ.

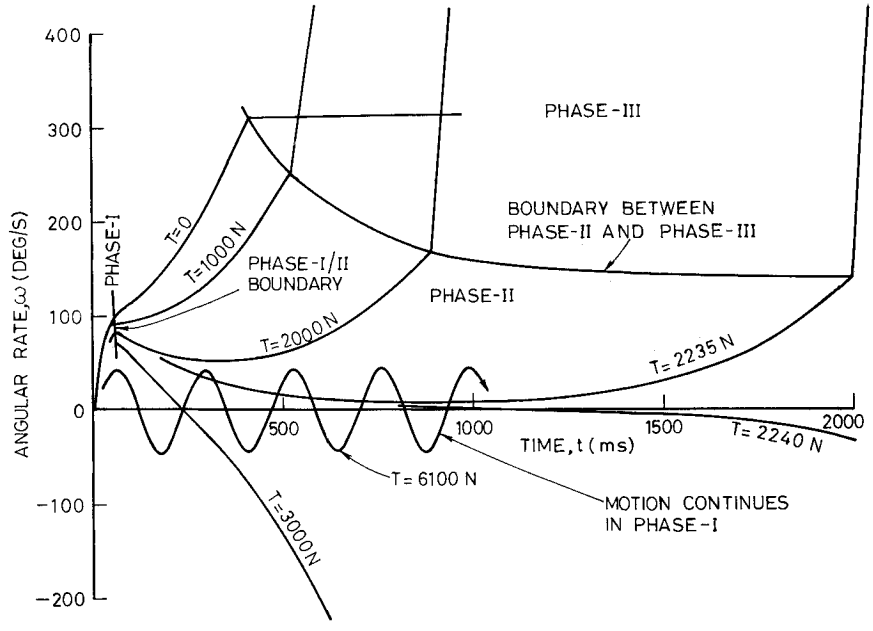

Fig. 8 Influence of residual thrust on evolution of angular rate ω.

Consider the critical situation for which

$$M_{c3} = ma\ell \sin(\bar{\theta} + \beta) \tag{34}$$

Then, solving the simultaneous Eqs. (33) and (34), we get the following transcendental equation in $\bar{\theta}$:

$$\bar{\theta} \sin(\bar{\theta} + \beta) + \cos(\bar{\theta} + \beta) = \cos\beta + 1/\zeta \tag{35}$$

This equation provides $\bar{\theta}$ as an implicit function of both the parameters β and ζ. We solve it numerically. The substitution of this $\bar{\theta}$ value in Eq. (34) enables us to obtain maximum permissible moment due to thrust.

Phase III

As before, in this phase too, the presence of residual thrust significantly complicates the equations of motion. Euler's equations of motion referred to the system center of mass now become

$$m\dot{v}_1 = T \sin(\theta - \alpha) \tag{36a}$$

$$m\dot{v}_2 = ma - T \cos(\theta - \alpha) \tag{36b}$$

$$I_c\ddot{\theta} = T\{\ell \sin(\alpha + \beta) - b \sin(\alpha + \varepsilon)\} \tag{36c}$$

These equations admit closed-form solutions in terms of Fresnel integrals,[14] however, here we use numerical integration to obtain solutions.

Finally, it may be worthwhile to normalize the three critical levels of moments appearing earlier in the course of formulation. On dividing these moments by $ma\ell$, we get the following dimensionless moments:

$$\hat{M}_{c1} = \sin\beta + 2/(\zeta\theta_1) \tag{37a}$$

$$\hat{M}_{c2} = \sin\beta + 1/2\,\theta_1\cos\beta + 1/(\zeta\theta_1) \tag{37b}$$

$$\hat{M}_{c3} = \sin(\bar{\theta} + \beta) \tag{37c}$$

These moments separate the three classes, each associated with its typical motion pattern. Evidently, the least of these, M_{c3}, is also the most important from the design viewpoint.

Results and Discussion

The methodology developed has now been utilized for the analysis of a typical system with relevant system parameters as indicated in Table 1. The related design parameters and some basic results are also included therein. The time history of the variables θ, ω, v_i, and R_i with $i = 1, 2$ in the absence of residual thrust is shown in Fig. 2. Under optimal conditions for which $\theta_2 = \theta_2^* = 32.956$ deg, the behavior of these variables is also presented. One observes that the lateral velocity component v_1 continually increases until θ attains this optimal value. However, the moment θ goes beyond, it starts falling with further increase in θ. It may be noted that the maximum v_1 occurs where the reaction R_1 vanishes. This numerically observed phenomenon is easily verified analytically through substitution of $\theta_2 = \theta_2^*$ in the expression for this reaction. Interestingly, it is also evident from Eq. (15a).

For a better comparative assessment of the influence of β, the corresponding results for $\beta = 0$ have been presented in Fig. 3. In general, a significant adverse influence of increasing β on the process of separation is indicated. Figure 4a shows the influence of the design parameter ζ and the angle β on the optimum value of the second angle. One observes that for $\zeta \leq 2/\cos\beta$, no meaningful optimal second angle exists since the lateral velocity component v_1 monotonically falls throughout the second phase. For larger ζ, θ_2^* initially builds up rapidly, however, it starts saturating soon after. The corresponding asymptotic value of θ_2^*, also available in the closed-form relation for the springless system, Eq. (22), plotted as a function of β is presented in Fig. 4b.

Figure 5 enables a clearer visualization of the general motion of the separating ullage system relative to the accelerating stage. Two cases with the optimal θ_2 ($= \theta_2^*$) and also for a nonoptimal θ_2 ($\neq \theta_2^*$) are considered. The paths traced by the system mass center as well as the lower end of the ullage frame are shown.

We now focus our attention on the effect of residual thrust, if any, on the separation process. Figure 6 presents the log-log plots showing the effects of design parameters ζ and θ_1 on the normalized critical moments, namely, $\hat{M}_{c1}$, $\hat{M}_{c2}$, and $\hat{M}_{c3}$. Two values of β have been considered. For the particular case when $\beta = 0$, the $\hat{M}_{c1}$, $\hat{M}_{c3}$ plots are linear throughout. However, $\hat{M}_{c2}$ exhibits this linearity on either side, whereas in the intermediate range of ζ, this curve is nonlinear. Evidently, the slopes for the extreme linear parts of the curve are different. A close scrutiny of the relations easily explains these observations. Needless to say, justification for the use of the log-log scale follows from the resulting much simpler plots. For a nonzero β, even on this scale, the linear behavior ceases to exist virtually in all cases. For low values of ζ, the moments $\hat{M}_{c1}$ and $\hat{M}_{c2}$ do not seem to show much dependence on β, whereas the most important moment $\hat{M}_{c3}$ falls significantly for the nonzero β considered for the typical example. For relatively larger values of ζ, the three moments saturate, approaching a common constant value.

The influence of residual thrust on the growth of state variables is shown in Figs. 7 and 8. As expected, an increase in the thrust causes the springs to take longer to relax and the phase I terminal angular rate to come down. The residual thrust continues to pull down the angular rate further whereas the moment due to the inertial force aids in the growth of angle θ. For residual thrust below the critical value ($T_{c3} = 2237$ N), the favorable effect eventually wins over the adverse thrust moment. However, if the thrust level exceeds this crucial limit, the ullage system first attains a zero angular velocity (at $\theta = \bar{\theta}$) and subsequently suffers a reversal of motion under the overpowering effect of this thrust. For small or modest thrust level excesses, since now $\theta \leq \bar{\theta} \leq \theta_2$, the hinge release does not take place and the ullage is sure to hit the core. The higher the residual thrust level is, the smaller would be the maximum angle ($\bar{\theta}$) attained by the ullage system. Now for the thrust exceeding the next critical level ($T_{c2} = 6044$ N), the system is unable even to cross beyond $\theta = \theta_1$ and thus is forced to stay in the first phase. The spring is never relaxed completely, resulting in persistent oscillations as discussed earlier. Such a typical case for $T = 6100$ N is also included in Figs. 7 and 8. The amplitude of oscillation Θ keeps falling as the thrust level is increased further and eventually, for the thrust level exceeding the next higher critical value ($T_{c1} = 11{,}098$ N), the separation motion does not commence at all. For a better appreciation of the system dynamics, the trajectories of the ullage rockets relative to the accelerating stage are presented for three subcritical cases of practical importance (Fig. 9).

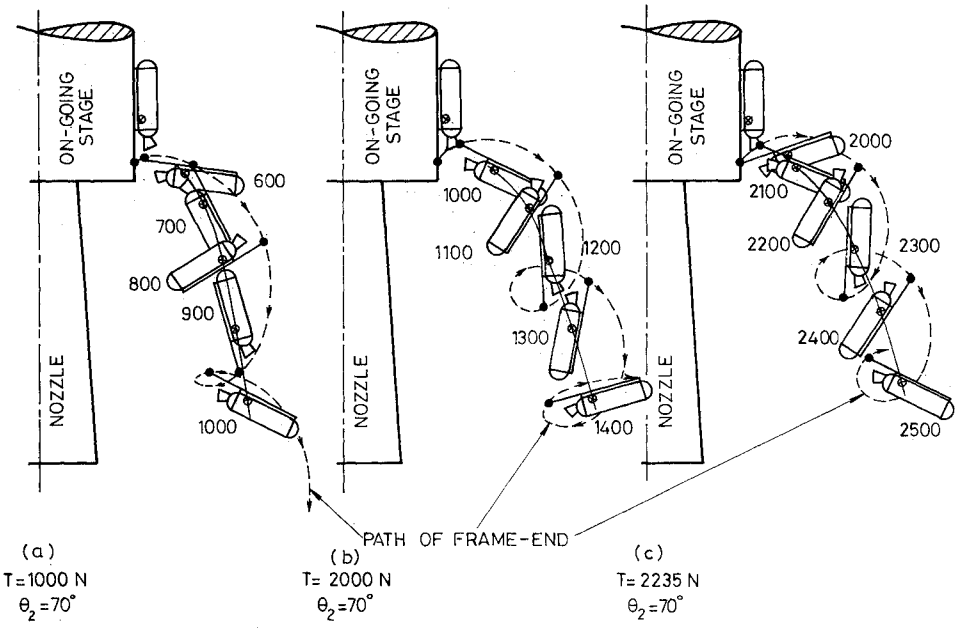

Fig. 9 Separation scenario in presence of leftover thrust.

Conclusions

The analysis presented here enables us to have a clear understanding of the various aspects of separation phenomena. Some important guidelines for the system design that emerge are as follows:

1) The location of the springs can be chosen arbitrarily within the various hardware constraints as long as the first angle remains small.

2) The angle at which the spent system gets released from the hinge should be chosen as close to the optimality condition as possible.

3) The acceleration of the thrusting stage and the residual thrust values are important inputs that have a significant influence on the separation system design.

A larger acceleration level is to be preferred whereas the residual thrust level must be minimized. A judicious system design must ensure that the thrust level remains well below the lowest critical value.

Acknowledgments

The authors would like to thank N. P. Giri and George Koshy at Vikram Sarabhai Space Center for many useful discussions on several hardware related aspects.

References

[1]Chubb, W., "The Collision Boundary Between the Two Separating Stages of the SA-4 Saturn Vehicles," NASA TN-D-598, Aug. 1961.

[2]Dwork, M., "Coning Effects Caused by Separation of Spin Stabilized Stages," *AIAA Journal*, Vol. 1, No. 11, 1963, pp. 2639, 2640.

[3]Wilke, R. O., "Comments on Coning Effects Caused by Separation of Spin Stabilized Stages," *AIAA Journal*, Vol. 2, No. 7, 1964, p. 1358.

[4]Waterfall, A. P., "A Theoretical Study of the Multispring Stage Separation System of the Black Arrow Satellite Launcher," Royal Aerospace Establishment, TR-682016, Farnborough Hants, England, UK, Aug. 1968.

[5]Longren, D. R., "Stage Separation Dynamics of Spin Stabilized Rockets," *Journal of Spacecraft and Rockets*, Vol. 7, No. 4, 1970, pp. 434–439.

[6]Subramanyam, J. D. A., "Separation Dynamics Analysis for a Multistage Rocket," *Proceedings of the International Symposium on Space Science and Technology*, edited by Shigeo Kobayashi, AGNE, Tokyo, Japan, 1973, pp. 383–390.

[7]Lochan, R., Sasidharan, K. G., and Biswas, K. K., "A Study on Separation Dynamics of APPLE," Indian Space Research Organisation, ISRO-VSSC-TR-15-78, Bangalore, India, July 1978.

[8]Lochan, R., Sasidharan, K. G., and Biswas, K. K., "Eulerian Analysis of Multistep Separation Dynamics," *Proceedings of the 23rd Congress of ISTAM*, edited by J. S. Rao, Globe Printers, Allahabad, India, 1978, pp. 38–48.

[9]Biswas, K. K., "Aspects of Non-Separating Apogee Motors," *Journal of Spacecraft and Rockets*, Vol. 21, No. 6, 1984, pp. 594–596.

[10]Sundaramurthy, H., Narayan, K. Y., Suryanarayana, G. K., Lochan, R., Sasidharan Nair, K. G., and Varambally, B. S., "Wind Tunnel Investigation of Strap-On Booster Separation Characteristics of a Launch Vehicle," *Journal of Aeronautical Society of India*, Vol. 38, No. 4, 1986, pp. 215–221.

[11]Biswas, K. K., "Some Aspects of Jettisoning Dynamics Related to Launch Vehicles," *Space Dynamics and Celestial Mechanics*, edited by K. B. Bhatnagar, Reidel, The Netherlands, 1986, pp. 369–379.

[12]Prahlad, T. S., "A Profile of Aerodynamic Research in VSSC with Application to Satellite Launch Vehicles," *Sadhana*, Vol. 12, Pts. 1 and 2, 1988, pp. 125–182.

[13]Lochan, R., Adimurthy, V., and Kumar, K., "Separation Dynamics of Strap-On Boosters," *Journal of Guidance, Control, and Dynamics*, Vol. 15, No. 1, 1992, pp. 137–143.

[14]Abramowitz, M., and Stegun, I. A., "Error Function and Fresnel Integrals," *Handbook of Mathematical Functions*, Dover, New York, 1965, pp. 297–309.